MISCELLANEOUS PAPER GL-79-11

LIQUEFACTION ANALYSIS FOR LACROSS NUCLEAR POWER STATION

by

William F. Marcuson III, Wayne A. Bieganousky

Geotechnical Laboratory
U. S. Army Engineer Waterways Experiment Station
P. O. Box 631, Vicksburg, Miss. 39180

June 1979

Final Report'

Approved For Public Release; Distribution Unlimited

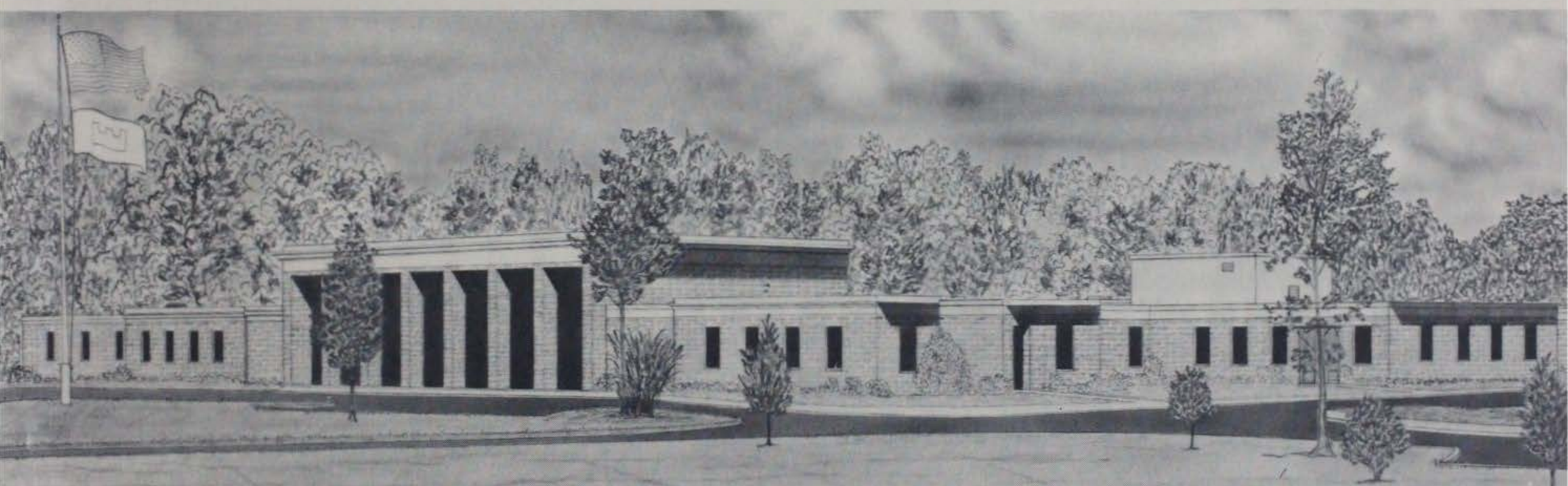

Prepared for U. S. Nuclear Regulatory Commission
Washington, D. C. 20555

Under Inter-Agency Agreement No. NRC-03-77-002

Unclassified

SECURITY CLASSIFICATION OF THIS PAGE *(When Data Entered)*

REPORT DOCUMENTATION PAGE

READ INSTRUCTIONS BEFORE COMPLETING FORM

1. REPORT NUMBER: Miscellaneous Paper GL-79-11

2. GOVT ACCESSION NO.:

3. RECIPIENT'S CATALOG NUMBER:

4. TITLE *(and Subtitle)*: LIQUEFACTION ANALYSIS FOR LACROSS NUCLEAR POWER STATION

5. TYPE OF REPORT & PERIOD COVERED: Final report

6. PERFORMING ORG. REPORT NUMBER:

7. AUTHOR(s): William F. Marcuson III, Wayne A. Bieganousky

8. CONTRACT OR GRANT NUMBER(s): Inter-Agency Agreement No. NRC-03-77-002

9. PERFORMING ORGANIZATION NAME AND ADDRESS: U. S. Army Engineer Waterways Experiment Station, Geotechnical Laboratory, P. O. Box 631, Vicksburg, Miss. 39180

10. PROGRAM ELEMENT, PROJECT, TASK AREA & WORK UNIT NUMBERS:

11. CONTROLLING OFFICE NAME AND ADDRESS: U. S. Nuclear Regulatory Commission, Washington, D. C. 20555

12. REPORT DATE: June 1979

13. NUMBER OF PAGES: 40

14. MONITORING AGENCY NAME & ADDRESS *(if different from Controlling Office)*:

15. SECURITY CLASS. *(of this report)*: Unclassified

15a. DECLASSIFICATION/DOWNGRADING SCHEDULE:

16. DISTRIBUTION STATEMENT *(of this Report)*: Approved for public release; distribution unlimited.

17. DISTRIBUTION STATEMENT *(of the abstract entered in Block 20, if different from Report)*:

18. SUPPLEMENTARY NOTES:

19. KEY WORDS *(Continue on reverse side if necessary and identify by block number)*:
Liquefaction
Nuclear power plant
Pile foundations
Soil mechanics

20. ABSTRACT *(Continue on reverse side if necessary and identify by block number)*:

The liquefaction potential of the LaCross site was evaluated for two earthquakes; namely, a safe shutdown earthquake (SSE) with a peak acceleration at the ground surface of 0.12 g, and an SSE with a peak acceleration at the ground surface of 0.2 g. The analysis was made by two methods: the Seed-Idriss Simplified Procedure and an empirical procedure. For a peak acceleration of 0.12 g, liquefaction is predicted by the Seed-Idriss calculations between a depth of 32 and 48 ft, and liquefaction is predicted by the empirical

(Continued)

DD FORM 1 JAN 73 1473 EDITION OF 1 NOV 65 IS OBSOLETE

Unclassified

SECURITY CLASSIFICATION OF THIS PAGE *(When Data Entered)*

20. Abstract (Continued)

method between a depth of 24 and 35 ft.

Assuming a peak acceleration of 0.2 g, the Seed-Idriss Simplified Procedure predicts liquefaction below a depth of 25 ft. The empirical method predicts liquefactions between a depth of 25 and 60 ft and between a depth of 85 and 115 ft.

The soils below the reactor at the LaCross site are predicted to strain badly, if an SSE which produces 0.12 g at the ground surface occurs; and are predicted to experience excessive strains and liquefaction if the SSE with a peak acceleration of 0.2 g occurs. Because of the limitations in the current state of knowledge concerning liquefaction and because of the limited data for use in this analysis, WES cannot conclude that the reactor vessel foundation is safe if the 0.12 g SSE occurs and concludes that the reactor vessel foundation is unsafe if the 0.2 g SSE occurs.

PREFACE

This report was prepared by the U. S. Army Engineer Waterways Experiment Station (WES) for the U. S. Nuclear Regulatory Commission (NRC) under the Consultant and Advisory Services in Geotechnical Engineering Project under Inter-Agency Agreement No. NRC-03-77-002.

The report was prepared during the period 1 August 1978 - 1 January 1979 by Dr. W. F. Marcuson, III, and Mr. W. A. Bieganousky of the Earthquake Engineering and Geophysics Division (EE&GD), Geotechnical Laboratory (GL), WES. The work was done under the general supervision of Dr. P. F. Hadala, Chief, EE&GD, and Mr. James P. Sale, Chief, GL.

Commander and Director of the WES during the preparation of this report was COL John L. Cannon, CE. Technical Director was Mr. F. R. Brown.

TABLE OF CONTENTS

CONVERSION FACTORS, U. S. CUSTOMARY TO METRIC (SI) UNITS OF MEASUREMENT

U. S. customary units of measurement used in this report can be converted to metric (SI) units as follows:

Multiply	By	To Obtain
inches	25.4	millimetres
feet	0.3048	metres
pounds (mass)	0.4535924	kilograms
pounds (mass) per cubic foot	16.01846	kilograms per cubic metre
pounds (force) per square inch	6894.757	pascals
pounds (force) per square foot	47.88026	pascals

LIQUEFACTION ANALYSIS FOR LACROSS NUCLEAR POWER STATION

Introduction

Background

1. The United States Nuclear Regulatory Commission (NRC) requested that the Waterways Experiment Station (WES) review certain foundation conditions at the LaCross Nuclear Station, an operating nuclear power plant. This plant, which is located near LaCross, Wisconsin, is among the oldest in the country and was put into operation before the present Site Analysis Report review system came into effect. This report documents WES' review of the LaCross Nuclear Station. Specifically, the question examined was the earthquake safety of the pile foundation which supports the containment vessel. The piles are driven through low to medium relative density sands and terminate in a dense sand layer approximately 28 ft* above bedrock.

Scope of work

2. The investigation of the foundation at the LaCross Nuclear Station included the following:

a. Review of Chapter 3, Soil Engineering Properties contained in the Application for Operating License for the LaCross Boiling Water Reactor by Dairyland Power Cooperative including portions of Appendix A, entitled "Field Exploration and Laboratory Tests,"[1] and associated design drawings.

b. The performance of a liquefaction analysis using the Seed-Idriss Simplified Procedure[2] assuming an earthquake with a peak acceleration of 0.12 and 0.2 g, respectively.

---

* A table for converting U. S. customary to metric (SI) units is given on page 3.

c. The performance of a liquefaction analysis using Seed's empirical method assuming both the 0.12 and 0.2 g earthquakes and comparison with a "rule of thumb" based on the Japanese experience at Niigata in 1964.

3. The objective of this study was to evaluate to the degree possible with the data available from prior field and laboratory studies by others, the seismic stability of the pile foundation which supports the containment vessel at the LaCross Nuclear Station.

Review of Previous Work

4. As stated earlier, portions of Reference 1 were reviewed to determine the soil profile under the containment vessel, including soil properties. Logs of Borings B-3 and B-4 drilled by Raymond International in July 1962 and Borings DM-1 and DM-3, drilled under Dames & Moore's supervision in 1973, were reviewed. Figure 1 shows an idealized soil profile in the vicinity of the reactor building. The ground surface is at elevation (el) 636 ft mean sea level (msl). The groundwater table was assumed at a depth of 13 ft. Top of bedrock is located at a depth of about 133 ft.

5. During construction, the soil was excavated to el 615 ft msl, and piles were driven below the reactor containment vessel. These piles terminated at el 535 ft. The piles were 50-ton cast in-place concrete piles with a tip diameter of 8 in., a butt diameter of 12 in. and an outer shell of 7-guage steel monotube, and were driven approximately 3-1/2 ft on centers. No mention was made of any internal reinforcing steel in the piles in the plans and reports provided to WES. A total of

approximately 230 piles were driven. The data provided indicate that the hammer used was a McKierman-Terry C-5 double-acting hammer with a rated striking energy of 16,000 ft-lb per blow. The piles were driven to at least a resistance of 6 blows per in. for the final 2 to 3 in. The number of blows in the last foot actually ranged from 75 to 330.

6. The soil below the reactor building (el 615) consisted of a fine to medium sand with occasional zones of clayey silt, coarse sand, and fine gravel, down to an elevation of approximately 535 ft. At el 535 ft, a 10-ft-thick fine to medium sand, with fine to medium gravels is encountered. Below this gravelly sandy layer, is an 18-ft-thick layer of sand which immediately overlies the bedrock.

7. Also shown on Figure 1 are the average blow counts, water content, dry and wet density, and shear-wave velocities for the six layers in the idealized soil profile. The reader is cautioned that the blow counts may or may not be Standard Penetration Test (SPT) N values. It was not explicitly stated in the available source of information how the penetration tests were conducted nor were they called "Standard Penetration Test" results. The values shown on Figure 1 are considered approximate average values for the layer. Both the blows per foot and the dry density values were obtained from an evaluation of the boring log data in Reference 1. The wet densities and shear-wave velocities which are shown on Figure 1 are estimates based on WES' experience and data presented in Reference 1.

8. Figure 2 is a plot of blows per foot versus depth. The data obtained in Boring B-3 are believed to have been obtained prior to pile

driving. The data obtained in Borings DM-1 and DM-2 are believed to have been obtained after pile driving. The reader is cautioned that a 1-to-1 comparison is impossible because the data obtained in Boring B-3 were obtained using a 2-in. split-spoon sampler while the data obtained in Borings DM-1 and DM-3 were obtained using the Dames & Moore sampler which is 3-1/4 in. in diameter. Figure 3 is the dry density information obtained from samples obtained from Borings DM-1 and DM-3.

9. Figure 4 is a plot of overburden pressure versus depth for the site. As stated previously, the water table was assumed at a depth of 13 ft. Below this depth both total and effective overburden pressures are shown.

10. The blow count values were assumed to be Standard Penetration Test N values and were used to compute relative density from the following equation:[3]

$$D_r = 11.7 + 0.76 \left[\left| 222(N) + 1600 - 53(\bar{\sigma}_o) - 50(C_u)^2 \right| \right]^{1/2} \qquad (1)$$

where

D_r = Relative density

N = Standard Penetration Test N values

$\bar{\sigma}_o$ = Effective overburden pressure in psi

C_u = The coefficient of uniformity

Using equation 1, the relative density of the top 105 ft is predicted to be between 50 and 60 percent.

11. Review of the available data[1] indicate that the material has the minimum density of about 100 pcf and a maximum density of about 120 pcf. These tests were run on bulk samples obtained by combining representative materials encountered at the site. WES' experience indicates that when

materials are combined the maximum and minimum density generally increase. This increase can be as much as 8 pcf. Consequently, WES believes that a minimum density of 92 pcf and a maximum density of 112 pcf may be more realistic for the in situ material. The relative densities predicted by equation 1 appear to be more nearly the same as those which would be obtained using the WES' maximum and minimum density estimates and the in situ dry unit weights given in Figure 3. An analysis of pile geometry records supplied by NRC suggest an average density increase of approximately 1 pcf due to pile driving. This is based on the reduction of void ratio which would occur assuming the soil displaced by the pile went entirely into taking up the voids of the adjacent soil. This assumes no soil heave and does not account for any densification due to vibrations during driving. An increase of 1 pcf is not significant and is believed not to contribute substantially to the stability of the soils. Records of ground surface movement during pile driving were sought but no such information was provided. While it is possible that more densification may have occurred, there were no data made available to WES which would support this hypothesis.

12. Dames & Moore determined the liquefaction potential of the subsurface soil by performing 11 stress-controlled dynamic triaxial compression tests on representative samples of the material considered to be potentially susceptible to liquefaction during the SSE. Eight of the samples were reconstituted to approximately what Dames & Moore believed to be the in situ density. In addition, three reconstituted samples were tested at slightly greater densities than the average in situ value (as determined by Dames & Moore) in order to examine the influence of density variation on liquefaction potential. These tests were run at confining

pressures of 1000 and 2000 psf and the results of these triaxial tests are shown on Figures 5 and 6. The data points identified by 104, 111, and 112 (the dry density in pcf) on Figure 5 were for specimens consolidated to an effective confining pressure of 1000 psf. The data identified by 106 and 105 (dry density in pcf) on Figure 6 were obtained by consolidating the specimens to an effective confining pressure of 2000 psf.

Dynamic Strength of the Soil

13. In order to evaluate the liquefaction potential of the soil in question, the laboratory cyclic triaxial test results obtained by Dames & Moore were used. Figures 5 and 6 are reproductions of Dames & Moore's test results. The as-tested dry densities of the remolded specimens made from material taken from Boring 5 at a depth of about 8-1/2 ft are shown next to the data points for these tests on Figure 5. A curve has been drawn through the data points for a dry density of about 111 pcf. As stated previously, WES believes that this material is at an in situ dry density of about 102 pcf. Consequently, a curve more or less parallel to the 111-lb curve was drawn through a data point at 104 pcf. This curve (marked γ_d = 102 pcf) was used to evaluate the soil strength. On Figure 6, the remolded soil specimens taken from Boring 3 at a depth of 35.5 ft have been used. Adjacent to each data point, the as-tested density is listed. A curve is drawn through these data for a density of about 106 pcf. A curve more or less parallel to this curve has been drawn and labeled γ_d = 100 pcf, because WES believes the in situ density of the material at a depth of about 38.5 is 100 pcf. This curve was also used to evaluate the dynamic soil strength.

14. As will be mentioned later on in this report, the number of equivalent cycles of load for SSE was chosen to be 10 (see discussion of design earthquake on page 8). Figures 5 and 6 were entered at 10 cycles and the stress ratio required to cause 10 percent double-amplitude strain was determined. This stress ratio was multiplied by 1000 and 2000 psf as appropriate to determine the superimposed dynamic shear strength. These values are plotted on Figure 7. A line was drawn through these data points and labeled isotropic laboratory data. Isotropically consolidated cyclic triaxial test data must be corrected by a correction factor, C_r , to represent field conditions. This correction factor is based on the comparison of cyclic triaxial test results to cyclic simple shear and SHAKE table test results (References 2, 4, and 5). For this investigation, a C_r of 0.57 was used. Also shown on Figure 7 is a curve labeled field conditions. The ordinate of this curve is 0.57 times the ordinate for the curve labeled isotropic laboratory data. The field condition curve was used to evaluate the dynamic shear strength of the soil during this investigation.

Seed-Idriss Simplified Procedure

15. In order to evaluate the liquefaction potential of a site, the cyclic stresses generated by the earthquake must be determined. Reference 2 suggests that the average shear stress, τ_{ave} , generated by an earthquake can be determined by the formula:

$$\tau_{ave} = 0.65 \times \frac{\gamma H}{g} A_{max} \times r_d \qquad (2)$$

where

γ = the total unit weight of the soil

H = depth from the ground surface to the point in question in feet

g = acceleration of gravity

A_{max} = the peak acceleration at the ground surface generated by the earthquake in the same system of units as g

r_d = a rigidity factor

The constant 0.65 is a factor which corrects the maximum shear stress to an equivalent sinusoidal shear stress.

16. Using equation 2, τ_{ave} can be determined for any depth in the soil profile. The r_d factor used in this analysis is shown by the curve marked "analysis" on Figure 8.

Earthquake parameters

17. In order to conduct this analysis, the maximum acceleration generated by the design earthquake and the number of equivalent cycles of stress are required. The maximum acceleration was specified by the NRC as 0.12 and 0.2 g. Review of the geological and seismological studies conducted at LaCross predict that an earthquake of Modified Mercalli Intensity VIII in the epicentral region has occurred on the Keweenaw fault.[1] For analysis purposes, an earthquake with an intensity one unit greater than the largest recorded intensity was assumed. Thus, using a Modified Mercalli Intensity of IX and using the intensity-magnitude relationships shown on Figure 9 (Reference 6), a magnitude 6.6 earthquake is postulated. Figure 10 is a plot of number of equivalent cycles versus magnitude which was developed by Seed.[5] This plot was entered and 10 equivalent cycles, which are essentially an upper bound

to the data in the plot, were assumed appropriate. For the design earthquakes (SSEa, and SSEb) 10 cycles and peak ground surface acceleration values of 0.12 and 0.2 g were used, respectively.

Analysis

18. Because of the high N values obtained in the dense sand layer at a depth of about 105 to 115 ft, this zone is predicted to remain stable even under the so-called design earthquakes. There are no other data available from this layer. If one assumes that the dynamic soil strength of this zone was the same as that judged appropriate for the upper materials by WES on Figure 7, then liquefaction might be predicted. WES does not believe this will happen.

SSE, 0.12 g

19. Table 1 presents the information needed to calculate the average shear stress (τ_{ave}) for the soil profile using the Seed-Idriss method.[2] Also listed on Table 1 is the effective overburden pressure ($\bar{\sigma}_o$) needed to enter Figure 7 to determine the available soil strength. Both the values of dynamic shear strength and dynamic shear stress are listed as a function of depth on Table 2. The factor of safety against 10 percent double-amplitude strain has been defined as the dynamic shear strength divided by the average dynamic shear stress. This factor of safety is also listed on Table 2. It should be noted that the factor of safety below a depth of 35 ft (depth of excavation) varies from 0.99 to 1.15 and is below 1.1 to a depth of 100 ft. Factors of safety less than 1 were predicted in the soil between a depth of 35 and 45 ft. It should be emphasized that the state of knowledge is not adequately refined and the assumptions required to carry out the analysis, given

the limitations in the existing data base, are such that it is not believed justified to call this site safe even though factors of safety marginally greater than 1 were calculated. However, this analysis does not prove the site unsafe under this acceleration as it is possible that had more extensive data and more thorough documentation been available, the judgments concerning the in-situ density and cyclic shear strength would have been different.

SSE, 0.2 g

20. The information needed to calculate τ_{ave} at the LaCross site for the SSE with 0.2 g peak acceleration is given on Table 3. Also shown on Table 3 is the effective overburden pressure which was used to enter Figure 7 to determine the shear strength of the soil. Table 4 presents the average shear stress and dynamic shear strength as a function of depth for this SSE. Also shown on Table 4 are factors of safety (as previously defined) for this SSE. As can be seen, the factors of safety below a depth of 35 ft vary from 0.59 to 0.66. Clearly, this indicates failure, as failure is defined in this report. A doubling of the cyclic strength over that shown by the authors would be required to produce a factor of safety of 1.25. This level is often considered reasonable for safety in the type of analysis performed herein.

Empirical Liquefaction Analysis

21. Empirical data in the form of stress ratio and corrected N values for sites that have and have not liquefied during past earthquakes, have been developed and plotted on Figure 11 (Reference 5). On Figure 11, the Standard Penetration Test N values have been corrected to an effective

overburden pressure of 1 tsf. As a second means to evaluate the liquefaction potential at the LaCross Site, the average blows per foot as shown on Figure 1, were plotted against the stress ratio and compared to the data shown on Figure 11. The stress ratio τ_{ave} divided by $\bar{\sigma}_o$ where $\bar{\sigma}_o$ is equal to the effective overburden pressure is also tabulated on Tables 1 and 3 for the various depths in question.

22. The blows per foot were assumed to be SPT N values and were corrected to an overburden pressure of 1 tsf by the formula:

$$N_1 = C_N \times N \tag{3}$$

where

N = Standard Penetration Test penetration resistance value measured in the field

N_1 = Standard Penetration Test N values corrected to an overburden pressure of 1 tsf

C_N = Correction factor

23. C_N was determined from Figure 12 (References 5 and 7). Figure 12 was extrapolated back to zero using data in Peck, Hanson, and Thornburn.[7] Values of C_N and N_1 are also shown on Tables 1 and 3. These values have been superimposed on Figure 11. Most of the values show that liquefaction should not occur; however, liquefaction is predicted from 25 to 35 ft.

24. A similar analysis was conducted assuming a SSE with a peak acceleration of 0.2 g. The stress ratios, C_N, N, and N_1, as a function of depth are tabulated on Table 3. These values are shown on Figure 13. These data indicate that liquefaction is possible if a SSE producing 0.2 g at the ground surface occurs. The data points to the far

right which indicate safe conditions are for the 10-ft-thick sand and gravel layer at a depth of about 105 ft where the piles end.

25. Based on the Japanese experience in the 16 June 1964 Niigata earthquake, a rule of thumb has been developed. This rule states that in order to be safe against liquefaction, the Standard Penetration Test N value should be at least two times the depth in meters.[8] A line has been drawn on Figure 2 indicating what the N value should be if it were greater than two times the depth in meters. Note that a large majority of the blows per foot fall on the unsafe side of this line. This is particularly important in this case since the peak acceleration at Niigata was approximately 0.16 g.

Summary and Conclusions

26. The liquefaction potential of the LaCross Site was evaluated for two earthquakes; namely, a SSE with a peak acceleration at the ground surface of 0.12 g, and a SSE with a peak acceleration at the ground surface of 0.2 g. The analysis was made by two methods; namely, the Seed-Idriss Simplified Procedure and an empirical procedure. Figure 14 is a summary plot of the dynamic shear stress as a function of depth for a peak acceleration of 0.12 g. Superimposed on this plot is a cyclic strength of the material assuming 10 equivalent cycles of loading. Note that liquefaction is predicted by the Seed-Idriss calculations between a depth of 32 and 48 ft and liquefaction is predicted by the empirical methods between a depth of 24 and 35 ft. Japanese experience at Niigata, Japan, also indicates that liquefaction would be predicted below a depth of 15 ft. As indicated in Appendix A, the piles could

support concentric static loads even after a loss of lateral support down to a depth of 48 ft. However, it would require dynamic structural analysis beyond the scope of this study to judge whether they would have sufficient bending resistance to withstand the transient eccentricity of the static vertical loading and the transient horizontal loads caused by the seismic excitation. In view of the fact that there appears to be no reinforcing bars in the top one-third of the pile[9] (as called for in some seismic design codes[10]), it is probable that the available bending resistance is modest.

27. Figure 15 is a summary plot of the dynamic shear stress as a function of depth for the soil profile assuming a peak acceleration of 0.2 g. Also shown on this plot is the dynamic shear strength of the soil assuming 10 equivalent cycles of loading. The Seed-Idriss Simplified Procedure predicts liquefaction below a depth of 25 ft. The empirical method predicts liquefaction between a depth of 25 and 60 ft and between a depth of 85 and 105 ft. If lateral support is lost in the depth ranges predicted by either method, the piles would be in danger of buckling failures as indicated in Appendix A.

28. Based on the judgments concerning the density and strength data and on analysis as presented herein, the soils below the reactor at the LaCross Site are predicted to strain badly if a SSE which produces 0.12 g at the surface of the soil occurs. The soils beneath the reactor vessel at the LaCross Site are predicted to experience excessive strains and liquefaction if the SSE with a peak acceleration at the ground surface of 0.2 g occurs. Because of the limitations in the current state of knowledge concerning liquefaction and because of the limited data available for use in this analysis, WES cannot conclude that the reactor

vessel foundation is safe if the 0.12 g SSE occurs and concludes that the reactor vessel foundation is unsafe if the 0.2 g SSE occurs.

References

1. Dairyland Power Cooperative, Application for Operating License for the LaCross Boiling Water Reactor.

2. Seed, H. B. and Idriss, I. M., "Simplified Procedure for Evaluating Soil Liquefaction Potential," Journal of the Soil Mechanics and Foundations Division, ASCE, Vol. 97, No. SM9, Proceedings Paper 8371, September 1971, pp. 1249-1273.

3. Marcuson, W. F., III and Bieganousky, W. A., "SPT and Relative Density in Coarse Sands," Journal of the Geotechnical Engineering Division, ASCE, Vol. 103, No. GT11, Proceedings Paper 13350, November 1977, pp. 1295-1309.

4. Seed, H. B. and Peacock, W. H., "Test Procedures for Measuring Soil Liquefaction Characteristics," Journal of the Soil Mechanics and Foundations Division, ASCE, Vol. 97, No. SM8, Proceedings Paper 8330, August 1971, pp. 1099-1119.

5. Seed, H. B., "Evaluation of Liquefaction Effects on Level Ground During Earthquakes," Preprint 2752, Liquefaction Problems in Geotechnical Engineering, ASCE National Convention and Exposition, Philadelphia, PA, 27 September - 1 October 1976, pp. 1-104.

6. Krinitzsky, E. L. and Chang, F. K., "State-of-the-Art for Assessing Earthquake Hazards in the United States; Earthquake Intensity and the Selection of Ground Motions for Seismic Design," Miscellaneous Paper S-73-1, Report 4, September 1975, U. S. Army Engineer Waterways Experiment Station, CE, Vicksburg, MS.

7. Peck, R. B., Hanson, W. E., and Thornburn, T. H., Foundation Engineering, New York, Wiley, 2nd Edition, p. 312.

8. Ohashi, M., Iwasaki, T., Tatsuoka, F., and Tokida, K., "A Practical Procedure for Assessing Earthquake-Induced Liquefaction of Sandy Deposits," Publics Works Research Institute Ministry of Construction, Tenth Joint Meeting U.S.-Japan Panel on Wind and Seismic Effects, UJNR, Washington, DC, 1978.

9. _____, "Containment Vessel Pile Driving Operations for 50 MWe Boiling Water Reactor at Genoa, Wisconsin," February 1963, Report No. SL-2003, Sargent and Lindy Engineers, Chicago, IL.

10. "Tentative Provision for the Development Seismic Regulation for Buildings", Applied Technology Command, Publication ATC 3-06, July 1978, U. S. Government Printing Office, Washington, DC, (P. 75, Section 7.5.3).

Table 1

LACROSS SITE LIQUEFACTION CALCULATIONS FOR A PEAK ACCELERATION OF 0.12 G

Middepth Sublayer	Depth ft	Overburden Pressure σ_o ksf	Effective Overburden Presure $\bar{\sigma}_o$ ksf	Octahedral Stress σ_{oct} ksf	Effective Octahedral Stress $\bar{\sigma}_{oct}$ ksf	Rigidity Factor r_d	Maximum Acceleration A_{max} % g	0.65 A_{max}	Average Shear Stress τ_{ave} ksf	Stress Ratio $\frac{\tau_{ave}}{\bar{\sigma}_o}$	Correction Factor C_N	SPT N Value N	Corrected SPT N Value N_1
1	2.5	0.273	0.273	0.182	0.182	1.0	0.12	0.078	0.021	0.078	1.48	9	13
2	7.5	0.818	0.818	0.545	0.545	0.99	0.12	0.078	0.063	0.077	1.28	9	12
3	11.5	1.254	1.254	0.836	0.836	0.98	0.12	0.078	0.096	0.076	1.18	9	11
4	14.0	1.535	1.473	1.023	0.982	0.97	0.12	0.078	0.116	0.079	1.11	9	10
5	17.5	1.948	1.667	1.299	1.111	0.96	0.12	0.078	0.146	0.088	1.03	8	8
6	22.5	2.538	1.945	1.692	1.297	0.95	0.12	0.078	0.188	0.097	0.96	8	8
7	27.5	3.128	2.223	2.085	1.482	0.94	0.12	0.078	0.229	0.103	0.95	8	8
8	32.5	3.718	2.501	2.479	1.667	0.91	0.12	0.078	0.264	0.106	0.90	8	7
9	37.5	4.308	2.779	2.872	1.853	0.88	0.12	0.078	0.296	0.106	0.85	16	14
10	42.5	4.898	3.057	3.265	2.038	0.84	0.12	0.078	0.321	0.105	0.81	16	13
11	47.5	5.488	3.335	3.659	2.223	0.80	0.12	0.078	0.342	0.103	0.77	16	12
12	52.5	6.078	3.613	4.052	2.409	0.77	0.12	0.078	0.365	0.101	0.74	16	12
13	57.5	6.668	3.891	4.445	2.594	0.74	0.12	0.078	0.385	0.99	0.71	16	11
14	62.5	7.276	4.187	4.851	2.791	0.73	0.12	0.078	0.414	0.099	0.68	25	17
15	67.5	7.901	4.500	5.267	3.000	0.71	0.12	0.078	0.438	0.097	0.65	25	16
16	72.5	8.526	4.813	5.684	3.209	0.70	0.12	0.078	0.465	0.097	0.62	25	16
17	77.5	9.151	5.126	6.101	3.417	0.69	0.12	0.078	0.493	0.096	0.60	25	15
18	82.5	9.776	5.439	6.517	3.626	0.68	0.12	0.078	0.519	0.095	0.58	25	15
19	87.5	10.401	5.752	6.934	3.835	0.67	0.12	0.078	0.544	0.095	0.55	25	14
20	92.5	11.026	6.065	7.351	4.043	0.66	0.12	0.078	0.568	0.094	0.54	25	14
21	97.5	11.651	6.378	7.767	4.252	0.65	0.12	0.078	0.591	0.093	0.53	25	13
22	102.5	12.276	6.691	8.184	4.461	0.64	0.12	0.078	0.613	0.092	0.51	25	13
23	107.5	12.921	7.029	8.617	4.686	0.63	0.12	0.078	0.635	0.090	0.50		
24	112.5	13.601	7.392	9.067	4.928	0.62	0.12	0.078	0.658	0.089	0.48		
25	117.5	14.251	7.730	9.501	5.153	0.61	0.12	0.078	0.678	0.088	0.47	60	28
26	122.5	14.876	8.043	9.917	5.362	0.61	0.12	0.078	0.708	0.088	0.46	60	28
27	127.5	15.501	8.356	10.334	5.571	0.60	0.12	0.078	0.725	0.087	0.45	60	27
28	131.5	16.001	8.606	10.667	5.737	0.60	0.12	0.078	0.749	0.087	0.44	60	26

Table 2

RESULTS OF DYNAMIC ANALYSIS 0.12 g SSE

Depth ft	Dynamic Shear Strength psf	Average Shear Stress τ_{ave}	Factor of Safety
2.5	50	21	2.38
7.5	102	63	1.62
11.5	145	96	1.51
14.0	166	116	1.43
17.5	185	146	1.27
22.5	212	188	1.13
27.5	239	229	1.04
32.5	293	296	0.99
42.5	320	321	0.99
47.5	347	342	1.02
52.5	374	365	1.02
57.5	400	385	1.04
62.5	429	414	1.04
67.5	460	438	1.05
72.5	490	465	1.05
77.5	520	493	1.05
82.5	551	519	1.06
87.5	581	544	1.07
92.5	611	568	1.08
97.5	642	591	1.09
102.5	672	613	1.10

Table 3

LACROSS SITE LIQUEFACTION CALCULATIONS FOR A PEAK ACCELERATION OF 0.20 G

Middepth Sublayer	Depth ft	Overburden Pressure σ_o ksf	Effective Overburden Pressure $\bar{\sigma}_o$ ksf	Octahedral Stress σ_{oct} ksf	Effective Octahedral Stress $\bar{\sigma}_{oct}$ ksf	Rigidity Factor r_d	Maximum Acceleration A_{max} %g	0.65 A_{max}	Average Shear Stress τ_{ave} ksf	Stress Ratio $\frac{\tau_{ave}}{\bar{\sigma}_o}$	Correction Factor C_N	SPT N Value N	Corrected SPT N Value N_1
1	2.5	0.273	0.273	0.182	0.182	1.0	0.20	0.13	0.036	0.132	1.48	9	13
2	7.5	0.818	0.818	0.545	0.545	0.99	0.20	0.13	0.105	0.128	1.28	9	12
3	11.5	1.254	1.254	0.836	0.836	0.98	0.20	0.13	0.160	0.128	1.18	9	11
4	14.0	1.535	1.473	1.023	0.982	0.97	0.20	0.13	0.194	0.132	1.11	9	10
5	17.5	1.948	1.667	1.299	1.111	0.96	0.20	0.13	0.243	0.146	1.03	8	8
6	22.5	2.538	1.945	1.692	1.297	0.95	0.20	0.13	0.313	0.161	0.96	8	8
7	27.5	3.128	2.223	2.085	1.482	0.94	0.20	0.13	0.382	0.172	0.95	8	8
8	32.5	3.718	2.501	2.479	1.667	0.91	0.20	0.13	0.440	0.176	0.90	8	7
9	37.5	4.308	2.779	2.872	1.853	0.88	0.20	0.13	0.493	0.177	0.85	16	14
10	42.5	4.898	3.057	3.265	2.038	0.84	0.20	0.13	0.535	0.175	0.81	16	13
11	47.5	5.488	3.335	3.659	2.223	0.80	0.20	0.13	0.571	0.171	0.77	16	12
12	52.5	6.078	3.613	4.052	2.409	0.77	0.20	0.13	0.608	0.168	0.74	16	12
13	57.5	6.668	3.891	4.445	2.594	0.74	0.20	0.13	0.641	0.165	0.71	16	11
14	62.5	7.276	4.187	4.851	2.791	0.73	0.20	0.13	0.690	0.165	0.68	25	17
15	67.5	7.901	4.500	5.267	3.000	0.71	0.20	0.13	0.729	0.162	0.65	25	16
16	72.5	8.526	4.813	5.684	3.209	0.70	0.20	0.13	0.776	0.161	0.62	25	16
17	77.5	9.151	5.126	6.101	3.417	0.69	0.20	0.13	0.821	0.160	0.60	25	15
18	82.5	9.776	5.439	6.517	3.626	0.68	0.20	0.13	0.864	0.159	0.58	25	15
19	87.5	10.401	5.752	6.934	3.835	0.67	0.20	0.13	0.905	0.157	0.55	25	14
20	92.5	11.026	6.065	7.351	4.043	0.66	0.20	0.13	0.946	0.156	0.54	25	14
21	97.5	11.651	6.378	7.767	4.252	0.65	0.20	0.13	0.984	0.154	0.53	25	13
22	102.5	12.276	6.691	8.184	4.461	0.64	0.20	0.13	1.021	0.152	0.51	25	13
23	107.5	12.926	7.029	8.617	4.686	0.63	0.20	0.13	1.058	0.151	0.50		
24	112.5	13.601	7.392	9.067	4.928	0.62	0.20	0.13	1.097	0.148	0.48		
25	117.5	14.251	7.730	9.501	5.153	0.61	0.20	0.13	1.130	0.146	0.47	60	28
26	122.5	14.876	8.043	9.917	5.362	0.61	0.20	0.13	1.180	0.147	0.46	60	28
27	127.5	15.501	8.356	10.334	5.571	0.60	0.20	0.13	1.209	0.145	0.45	60	27
28	131.5	16.001	8.606	10.667	5.737	0.60	0.20	0.13	1.248	0.145	0.44	60	26

Table 4

DYNAMIC ANALYSIS FOR 0.20 g SSE

Depth ft	Dynamic Shear Stress psf	Average Shear Stress τ_{ave}	Factor of Safety
2.5	50	30	1.39
7.5	102	105	0.97
11.5	145	160	0.91
14.0	166	194	0.86
17.5	185	243	0.76
22.5	212	313	0.68
27.5	239	382	0.63
32.5	266	440	0.60
37.5	293	493	0.59
42.5	320	535	0.60
47.5	347	571	0.61
52.5	374	608	0.61
57.5	400	641	0.62
62.5	429	690	0.62
67.5	460	729	0.63
72.5	490	776	0.63
77.5	520	821	0.63
82.5	551	864	0.64
87.5	581	905	0.64
92.5	611	946	0.65
97.5	642	984	0.65
102.5	672	1021	0.66

Elev	Z(ft)		N (Blows/ft)	w%	γ_{DRY} (PCF)	γ_{WET} (PCF)	V_s (fps)
640	0	G.S. EL 639					
		① Hydraulic fill – Brown fine to medium Sand, occasional fine gravel.	9	6.8	102.0	109.0 *118.0	300
630	10	13' ▽ WATER TABLE					
620	20	② Brown or grey fine to medium fine Sand, some thin seams of black clayey silt	8	19.5	98.0	118.0	300
610	30	Nominal bottom of excavation 35'					
600	40	③ Brown fine to medium Sand, occasional zones of coarse sand/ fine gravel, with < 5% silt	16		102.0	*118.0	350
590	50						
580	60	60'					
570	70	④ Brown fine to medium Sand, occasional zones of coarse sand/ fine gravel, with < 5% silt	25		107.0	*125.0	500
560	80						
550	90						
540	100	Nominal base of piles 105'					
530	110	⑤ Brown fine or fine to medium Sand, fine to medium gravel			118.0	*135.0	800
		115'					
520	120	⑥ Brown fine or fine to medium Sand, traces of silt, occasional gravel zones	60		110.0	*125.0	650
510	130	133'					
500	140						2500

* Assumed based on Terzaghi & Peck

Figure 1. Idealized Soil Profile and Approximate Average Values Assigned to Each Layer for Analysis

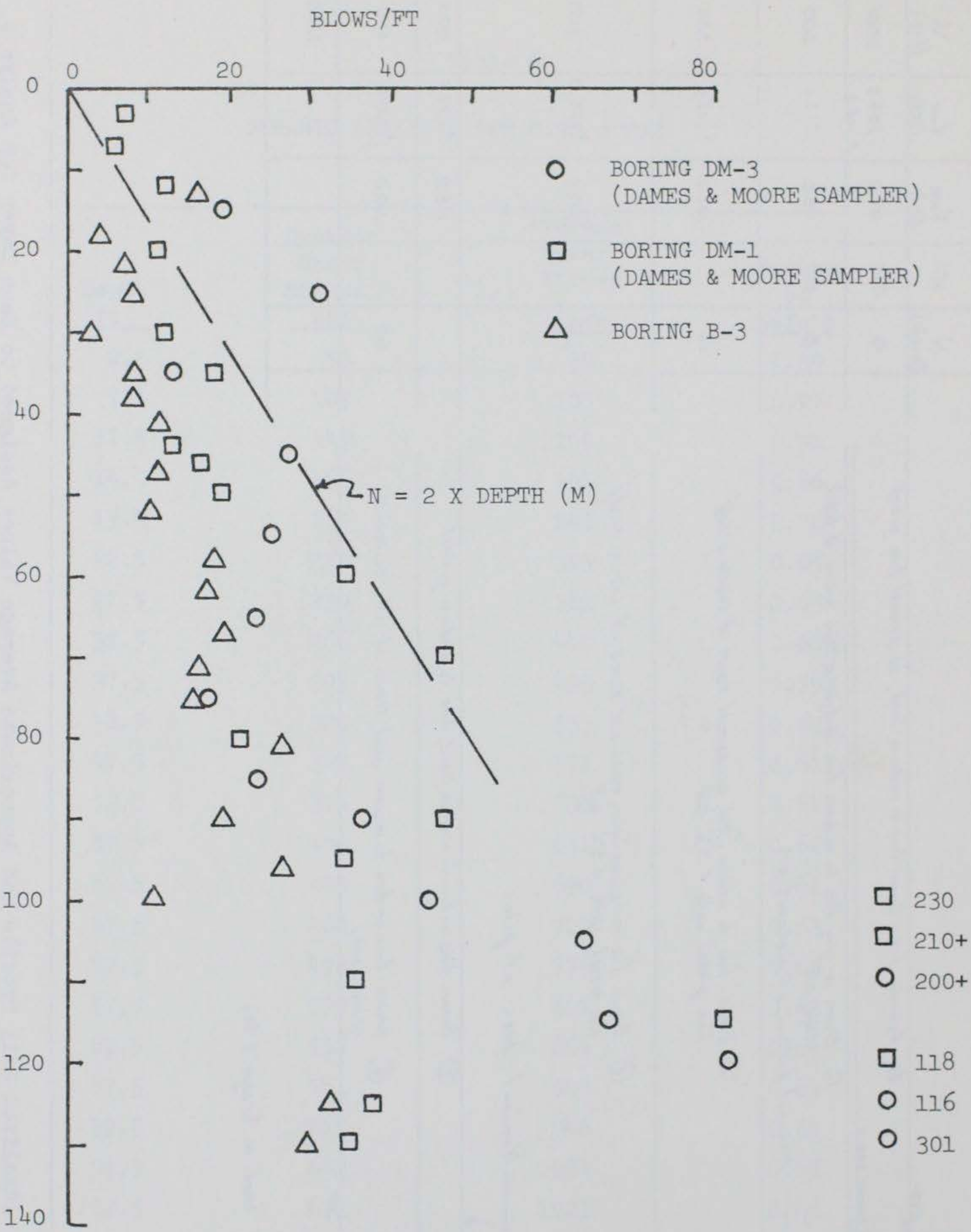

Figure 2. Blow Counts Presented as a Function of Depth

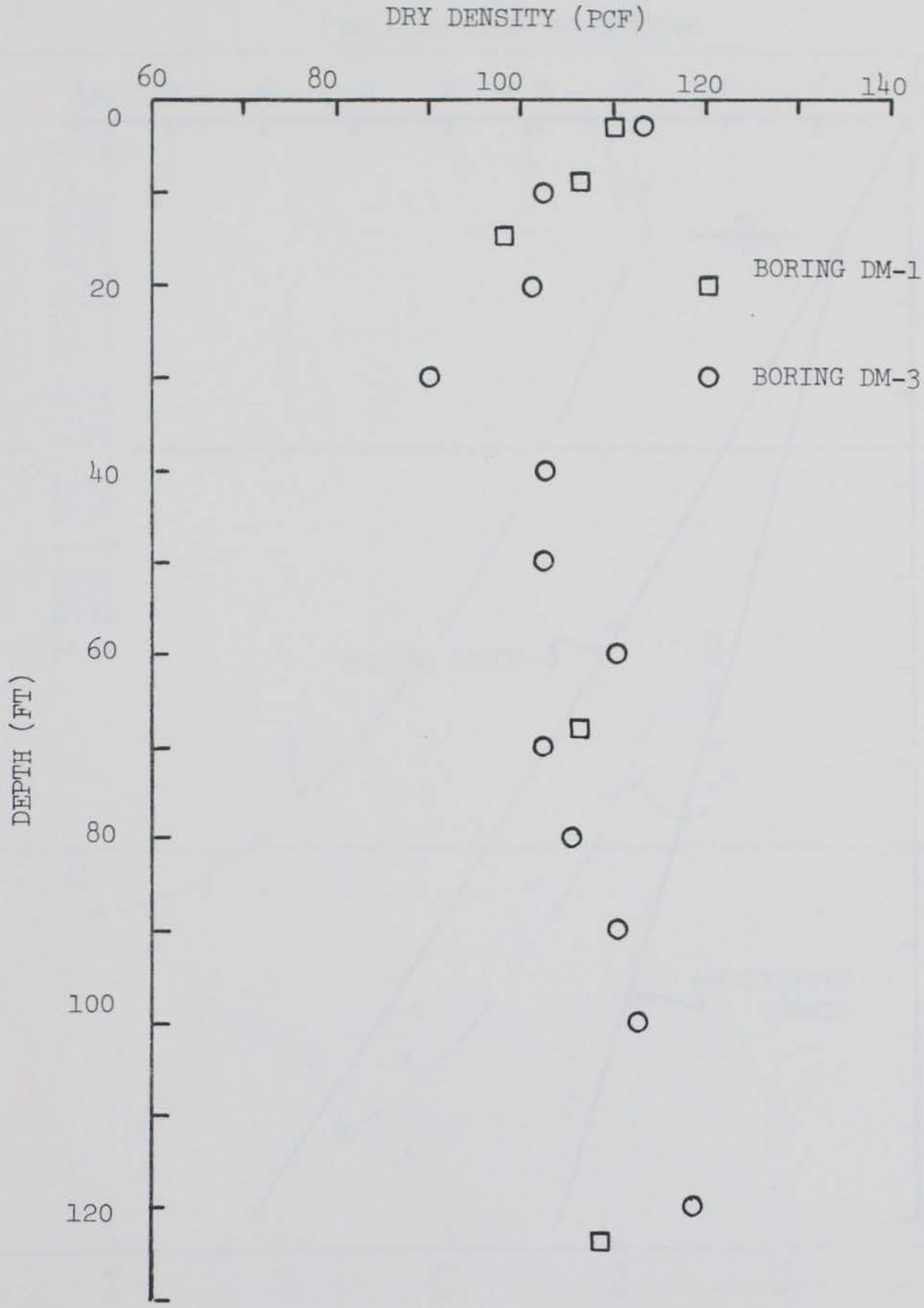

Figure 3. Dry Density as a Function of Depth

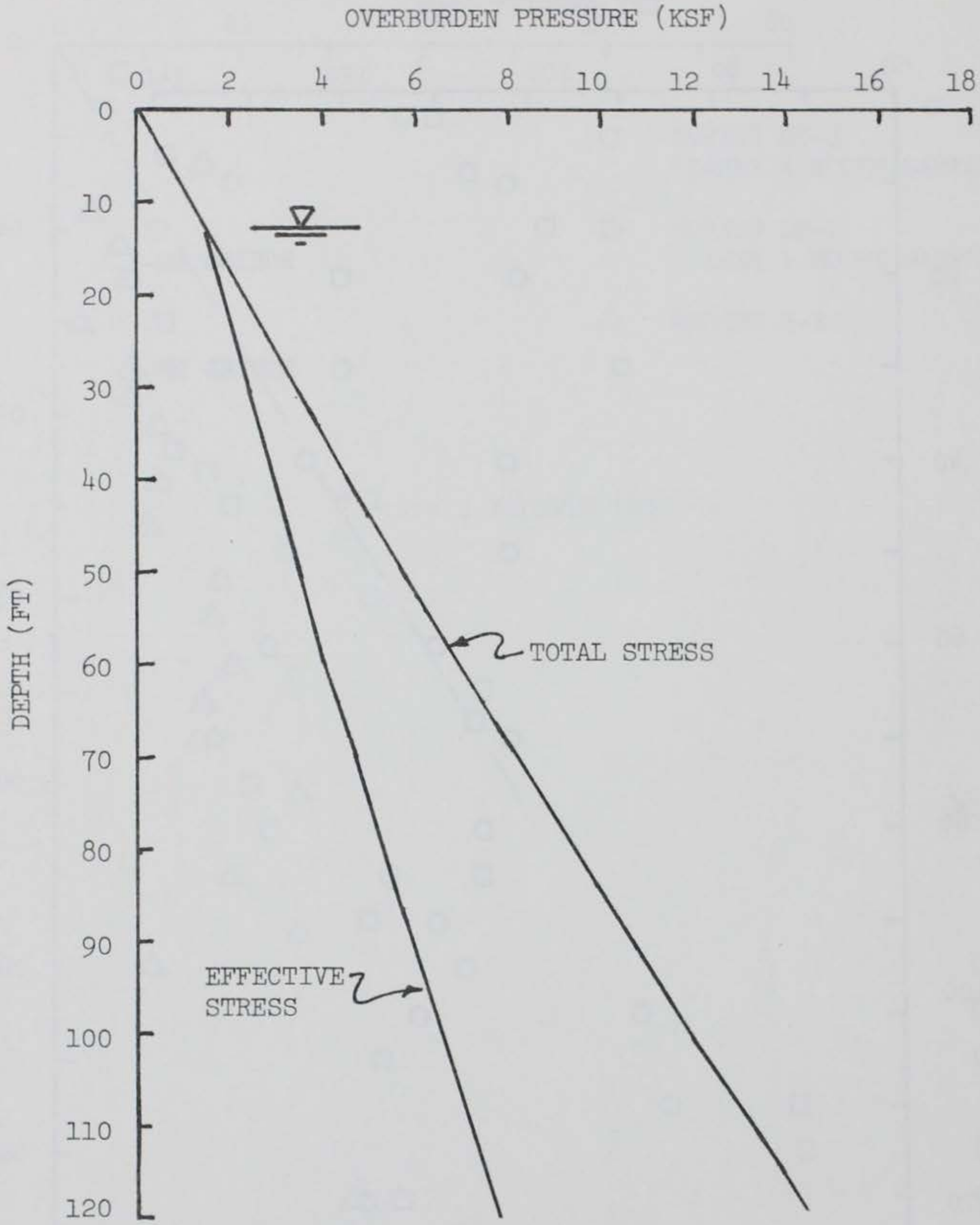

Figure 4. Overburden Pressure Versus Depth

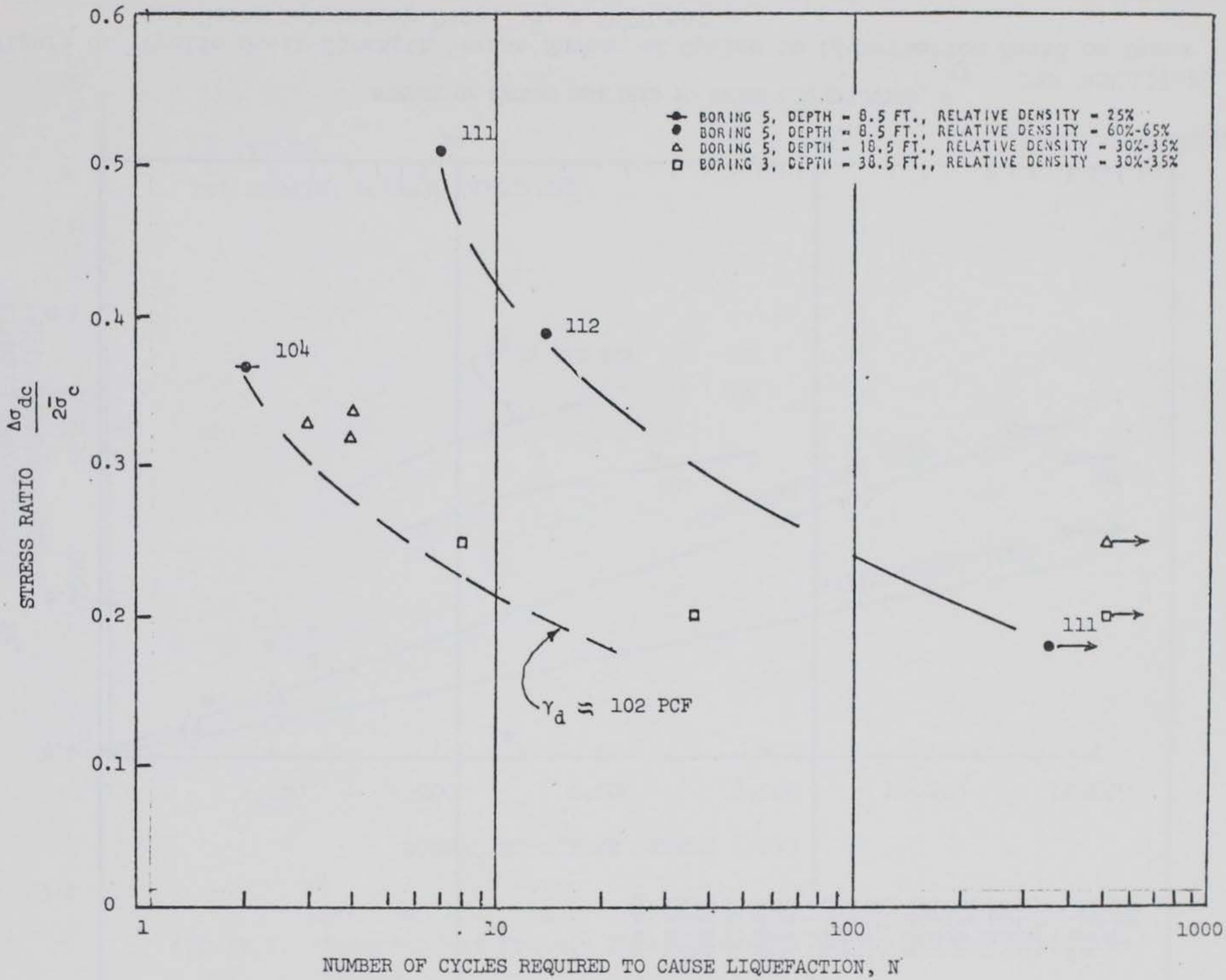

Figure 5. Cyclic Shear Strength Versus Number of Cycles to Liquefaction Based on Dames and Moore Laboratory Data, $\bar{\sigma}_c$ = 1000 psf

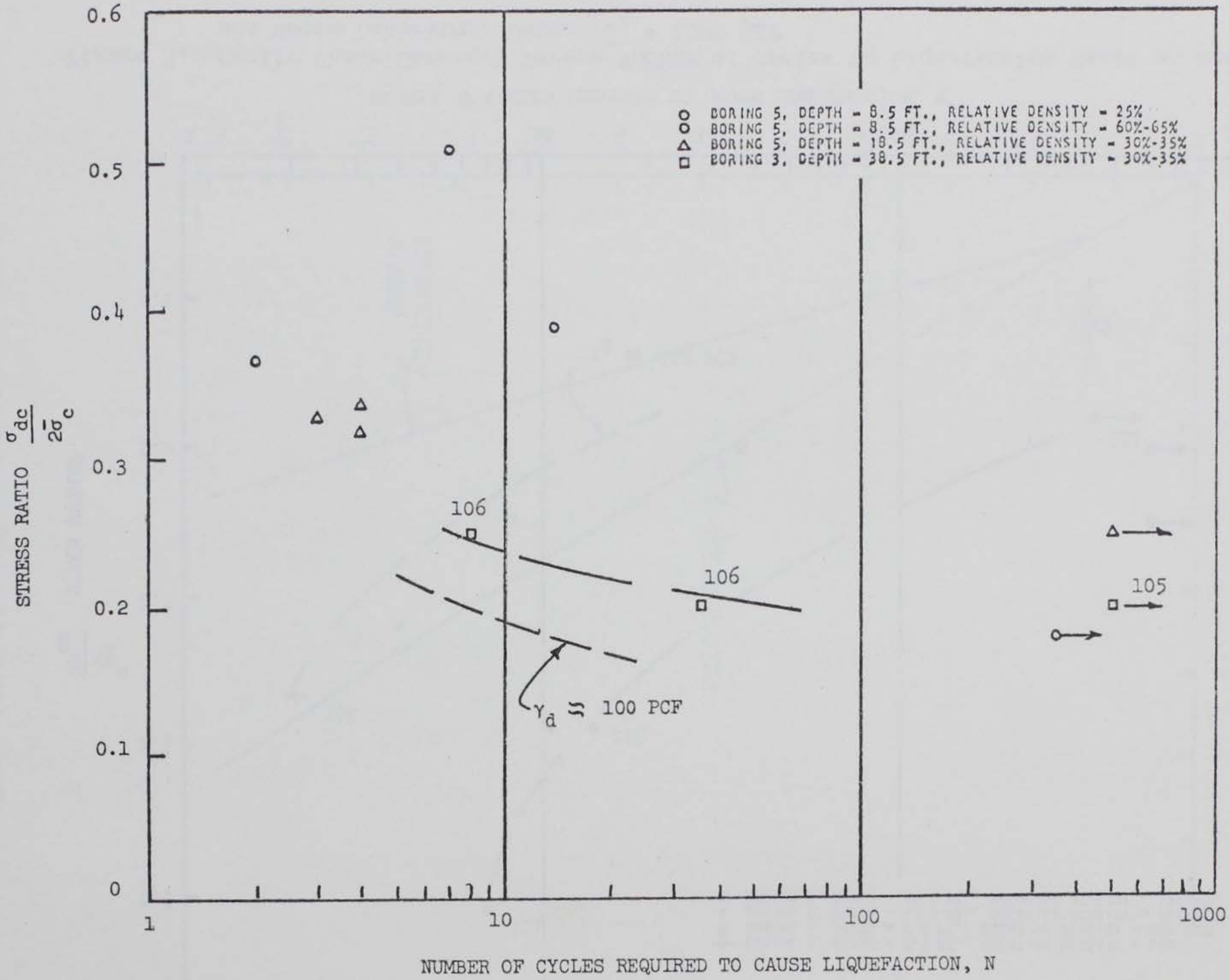

Figure 6. Cyclic Shear Strength Versus Number of Cycles to Liquefaction Based on Dames and Moore Laboratory Data, $\bar{\sigma}_c$ = 2000 psf

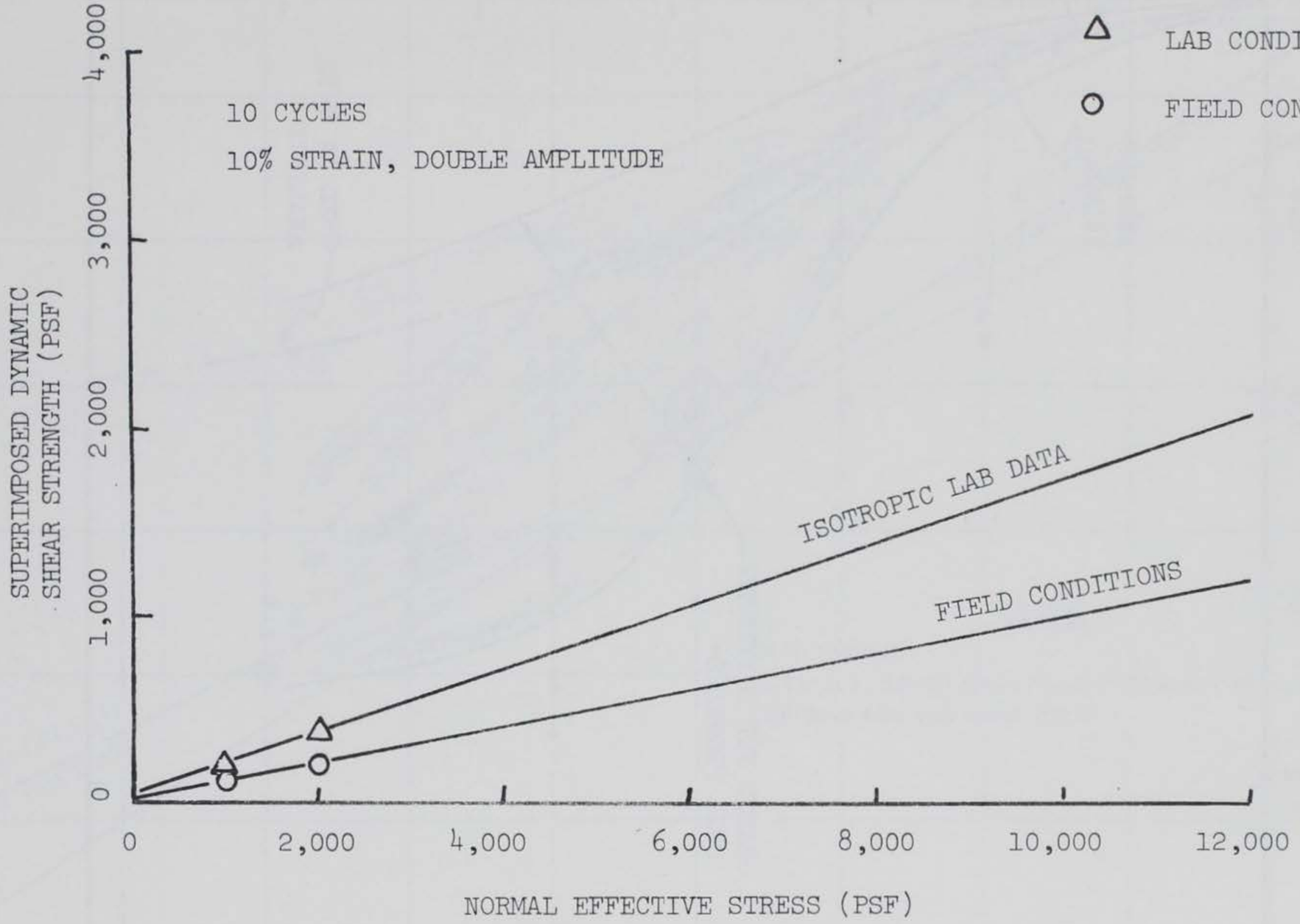

Figure 7. Superimposed Dynamic Shear Strength Versus Normal Effective Stress

$$r_d = \frac{(\tau_{max})_d}{(\tau_{max})_n}$$

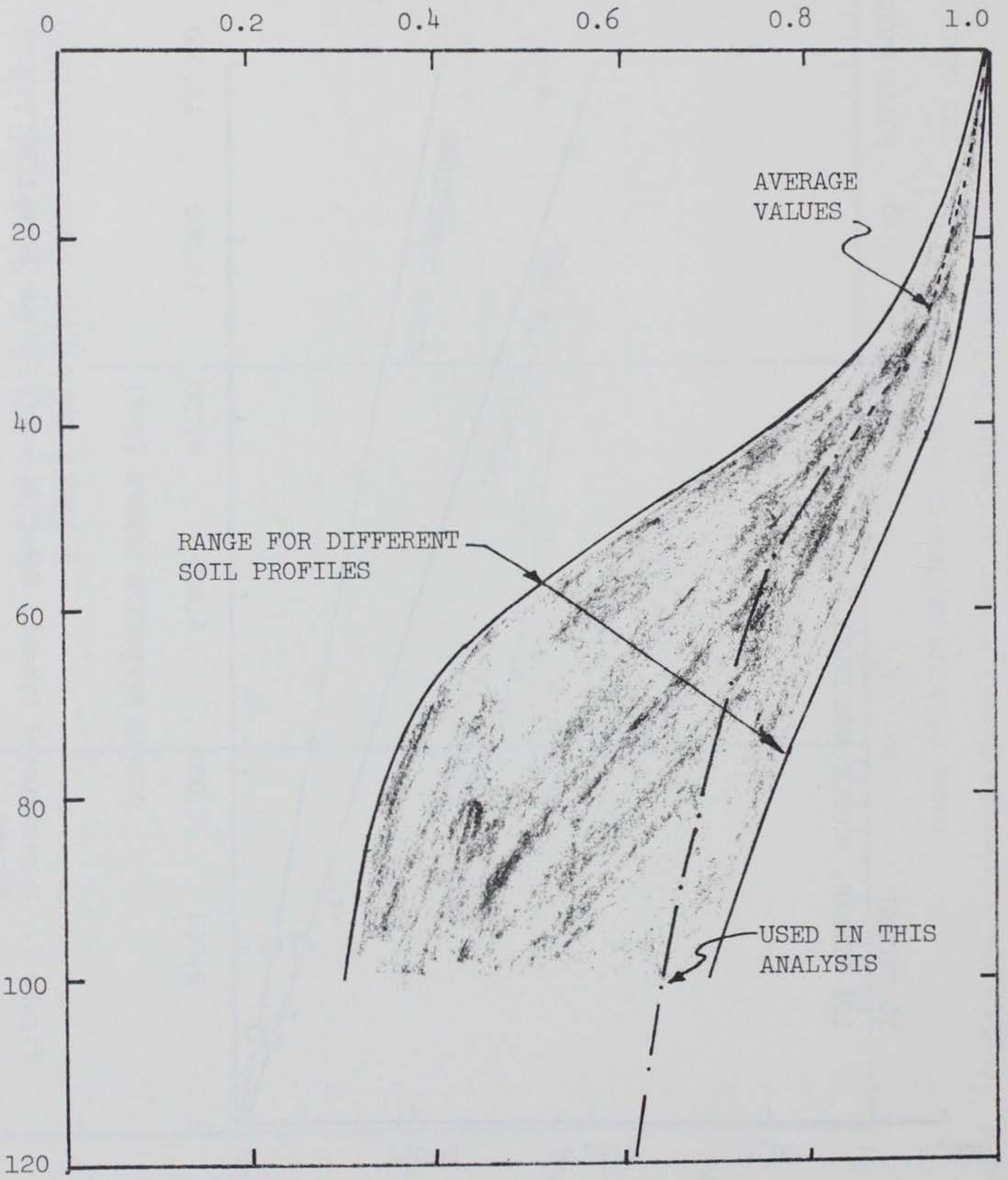

Figure 8. Rigidity Factor Versus Depth (after Reference 2)

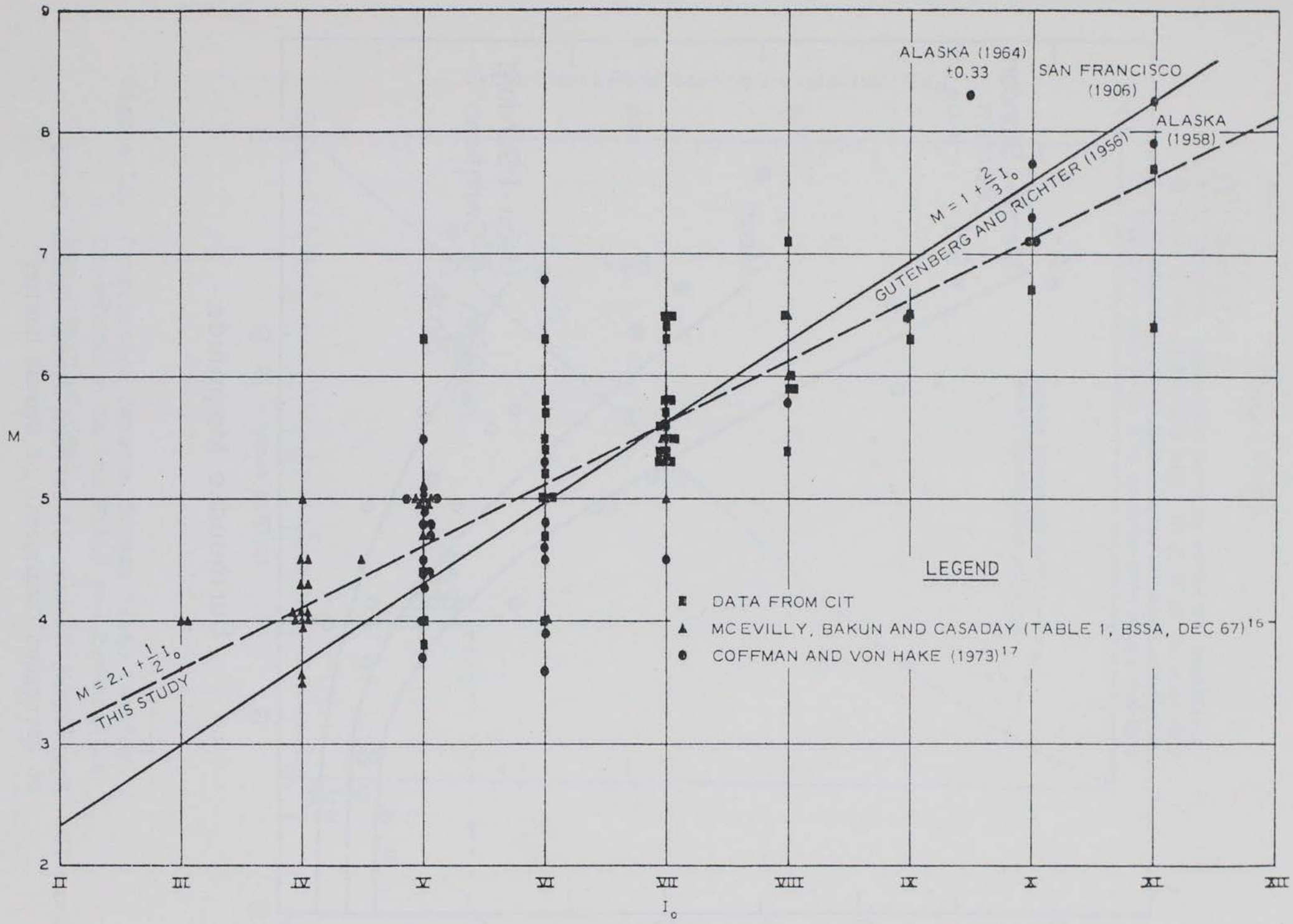

Figure 9. Relation Between Earthquake Magnitude and Intensity in Western United States (after Reference 6)

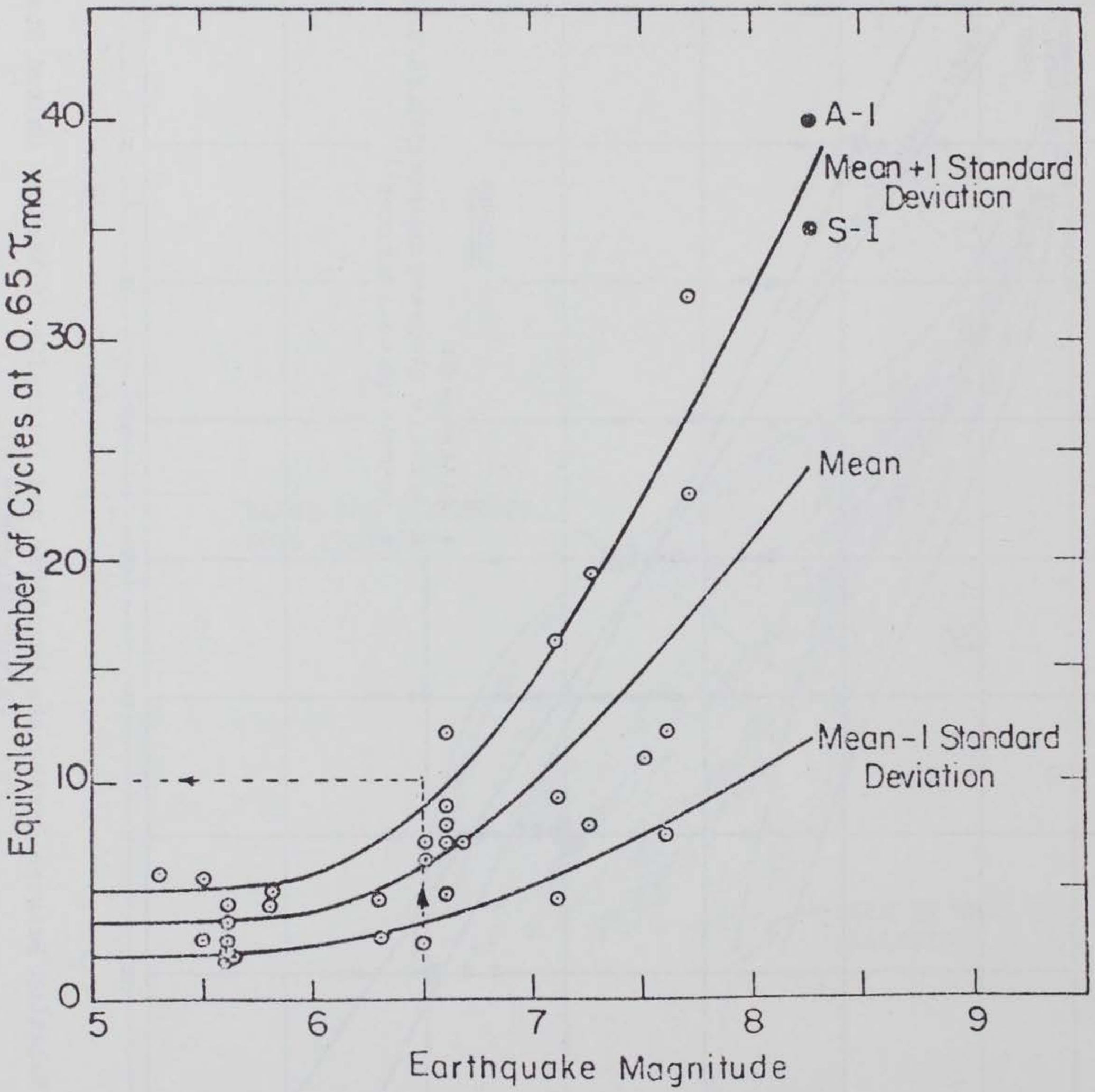

Figure 10. Equivalent Numbers of Uniform Stress Cycles Based on Strongest Components of Ground Motion

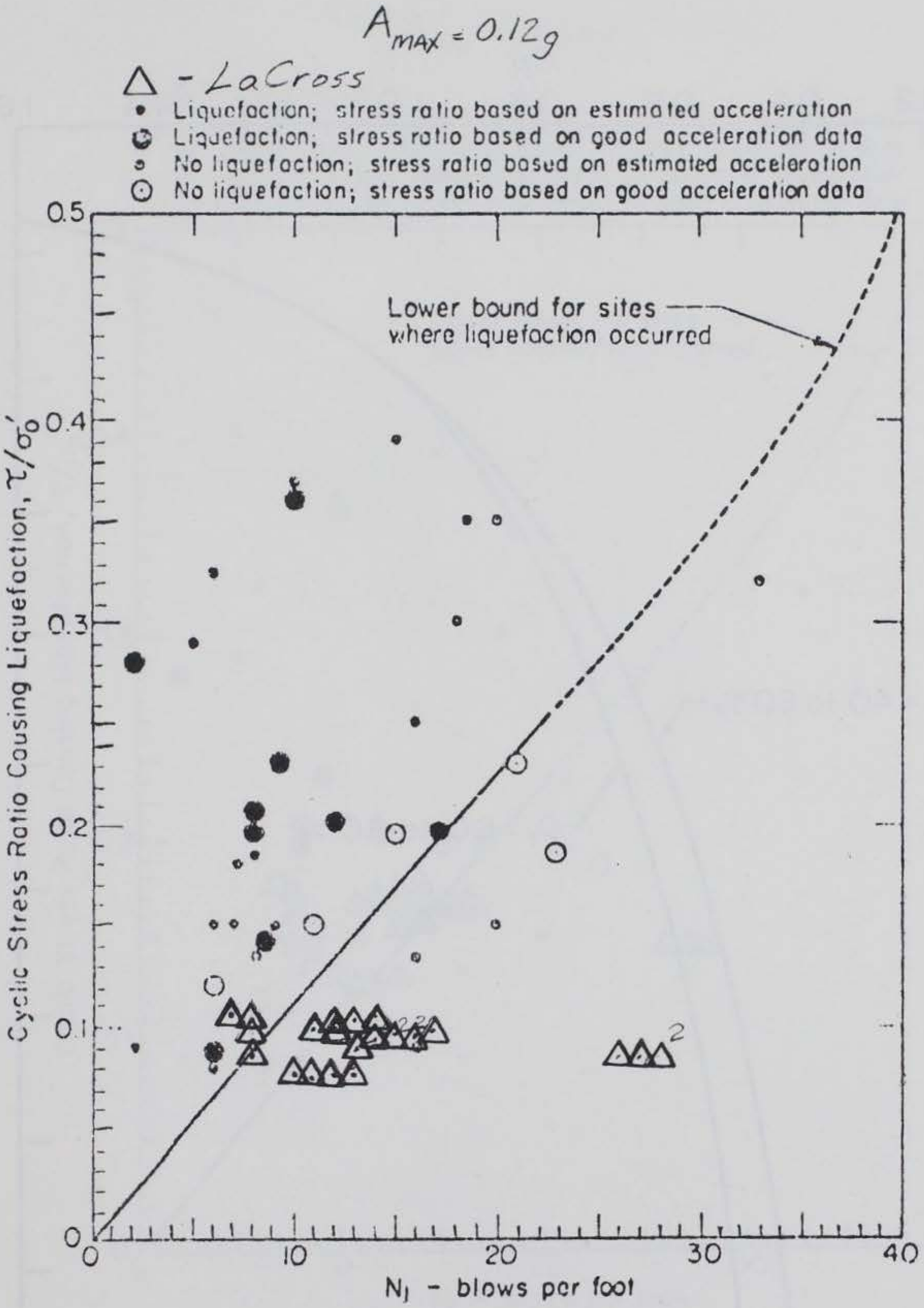

Figure 11. Correlation Between Stress Ratio Causing Liquefaction in the Field and Penetration Resistance of Sand

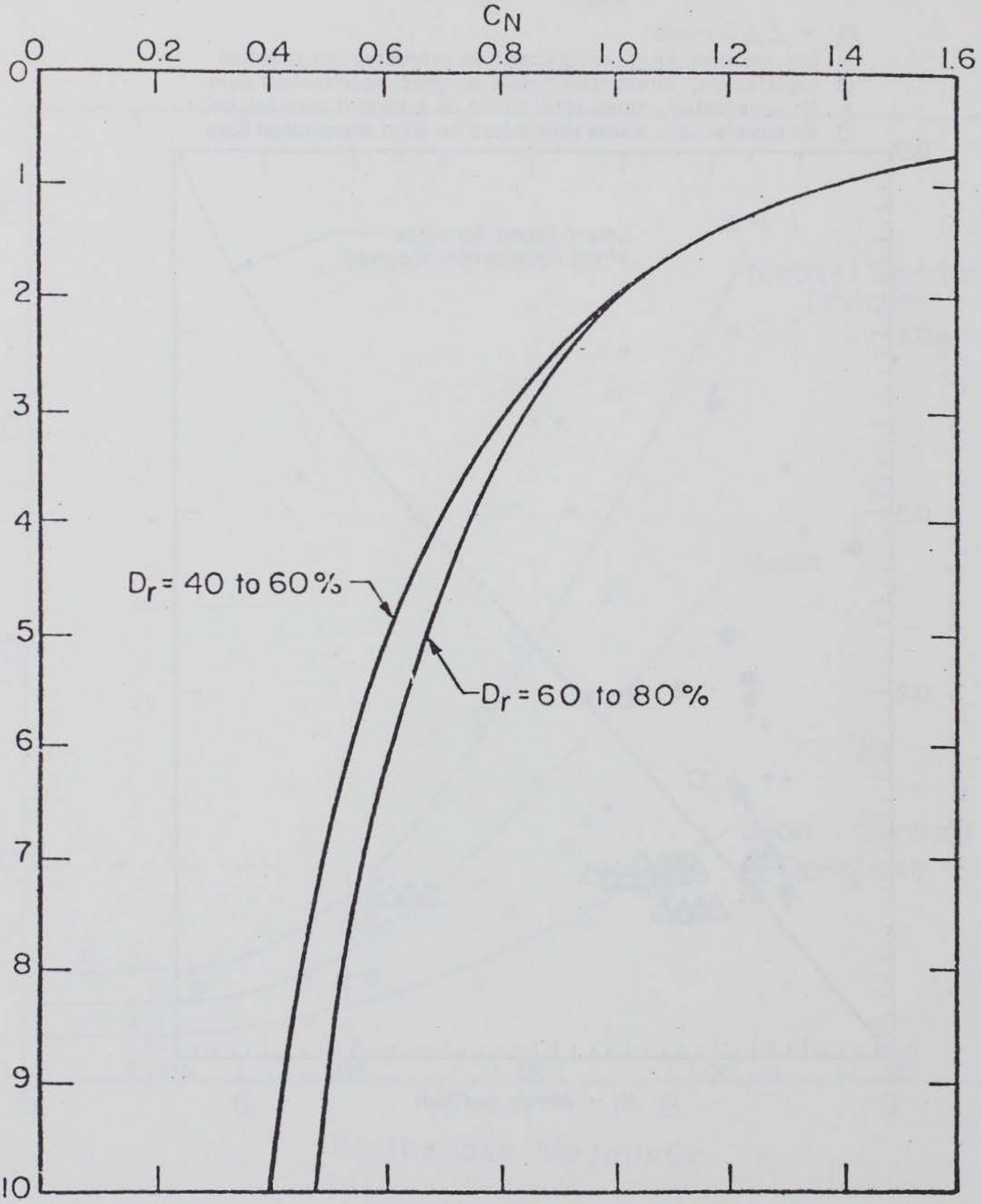

Figure 12. Recommended Curves for Determination of C_N Based on Averages for WES Tests (After Reference 5)

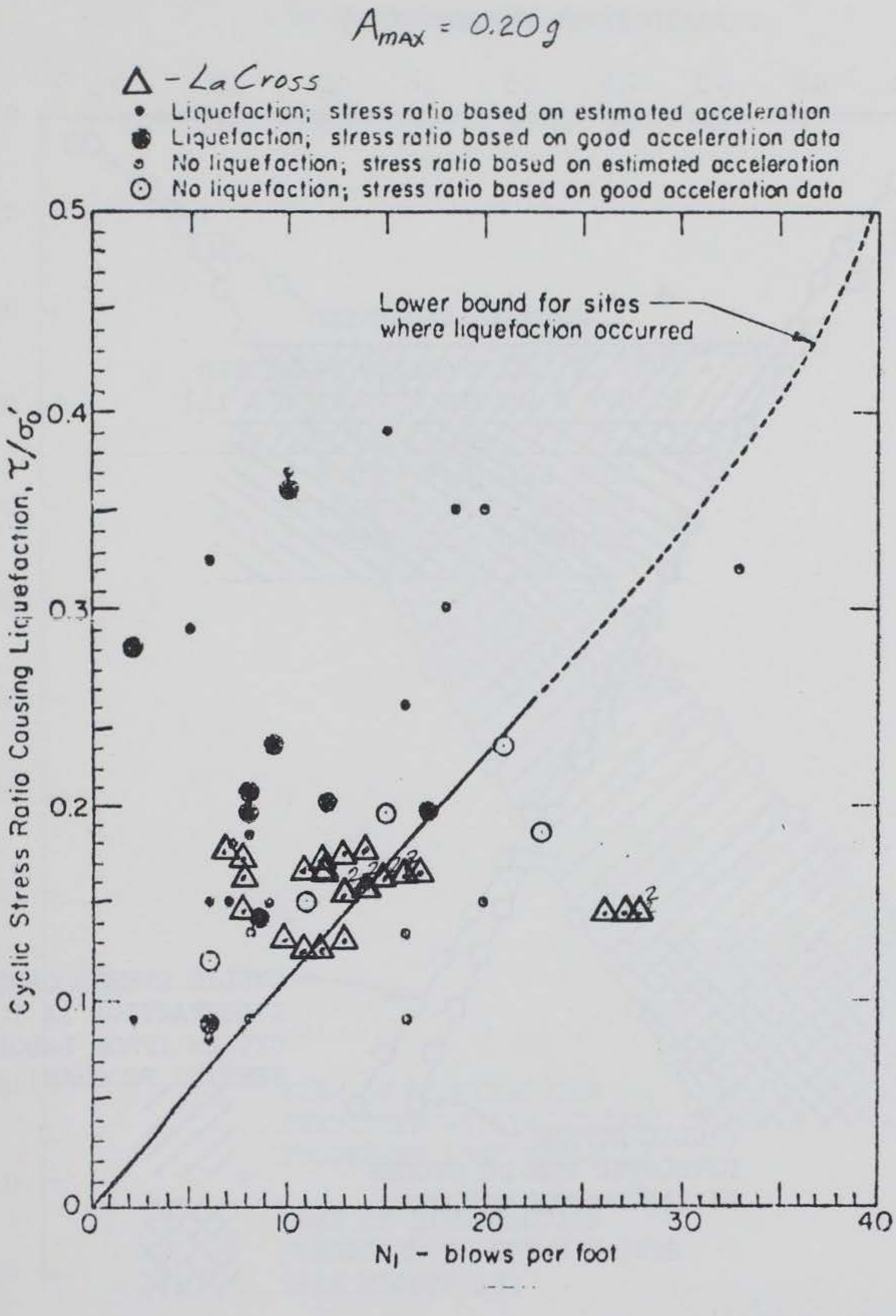

Figure 13. Correlation Between Stress Ratio Causing Liquefaction in the Field and Penetration Resistance of Sand

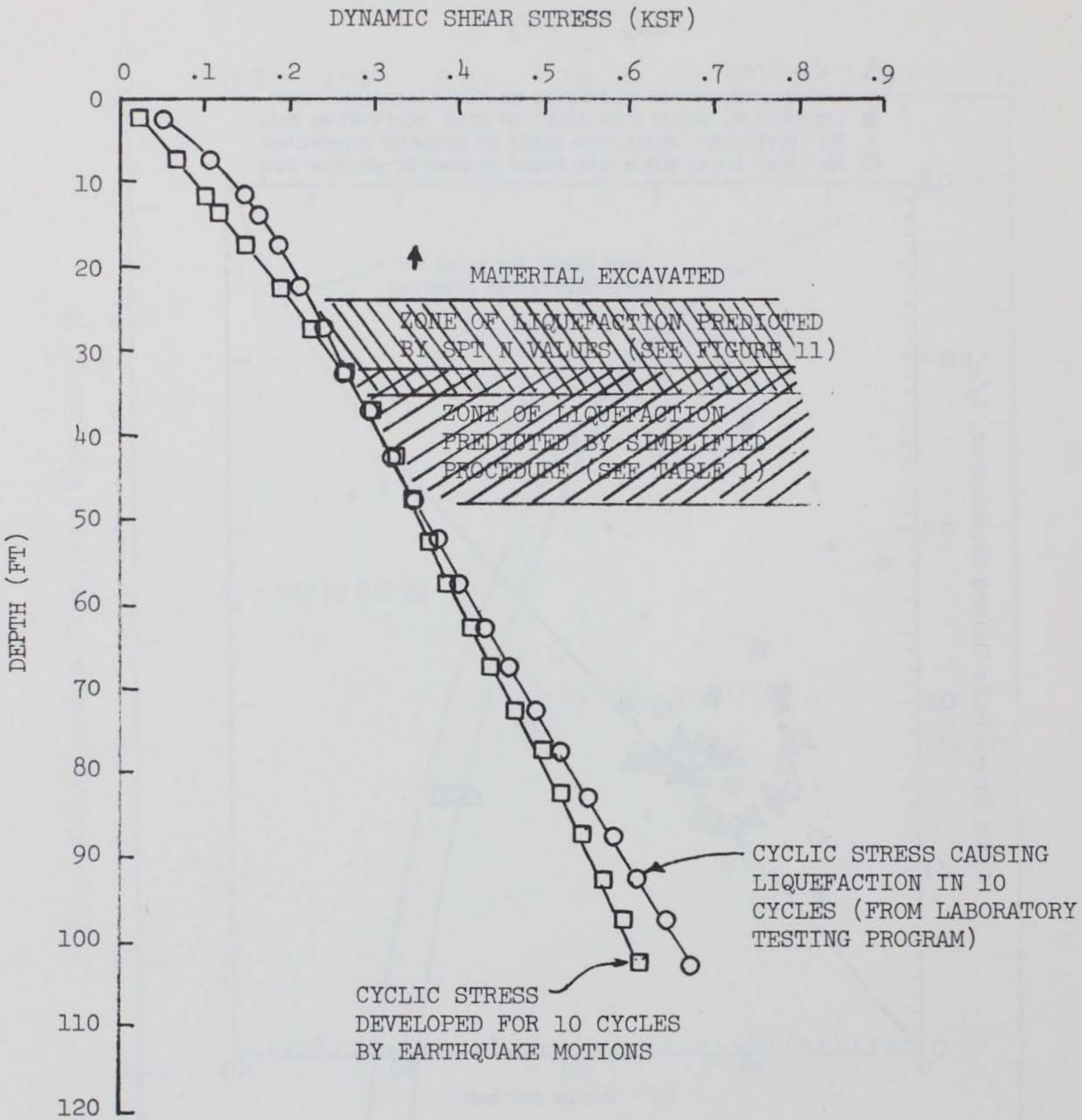

Figure 14. Results of SPT Empirical Study for SSE = 0.12 G

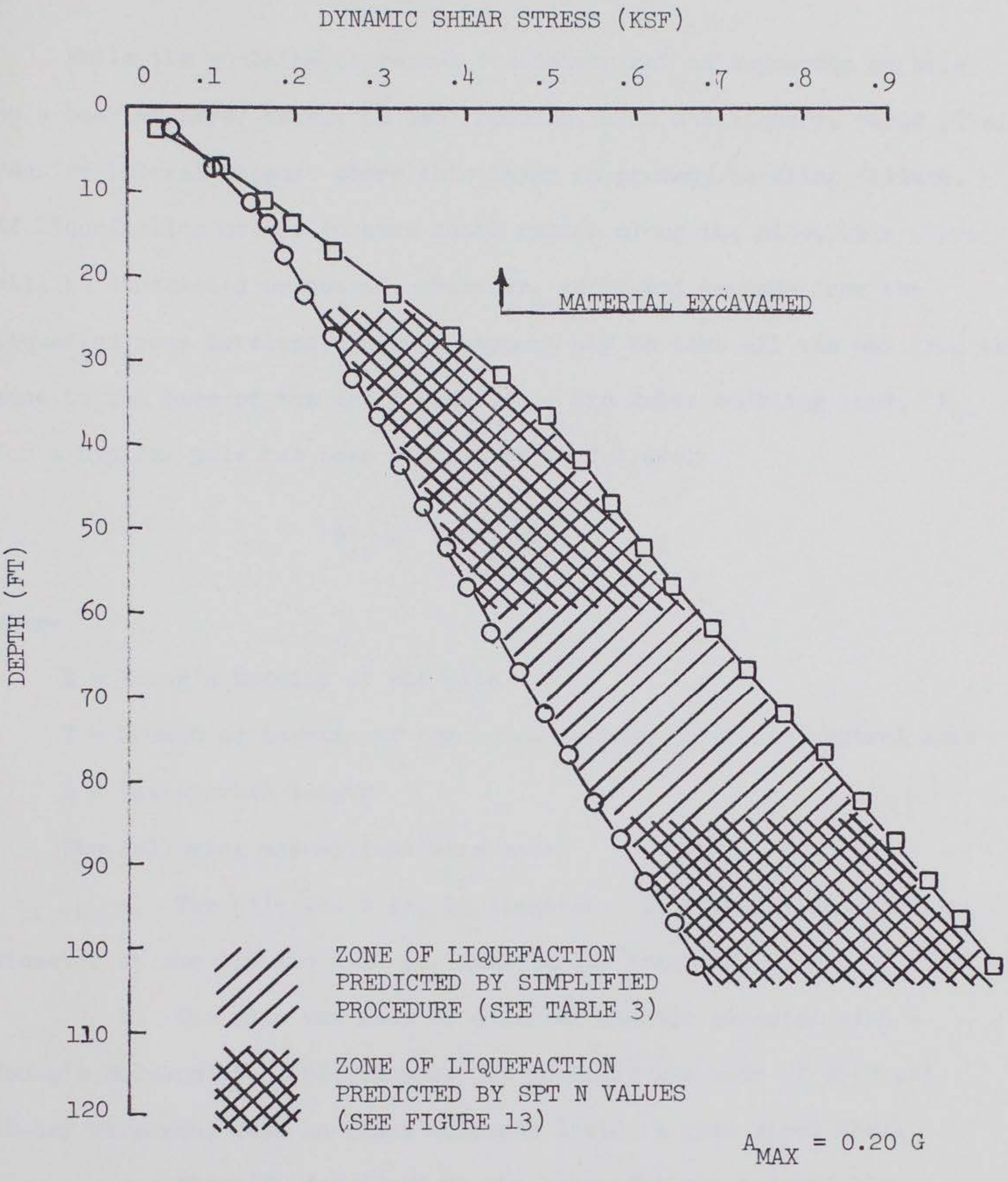

Figure 15. Results of SPT Empirical Study for SSE = 0.20 G

APPENDIX A

CALCULATION OF BUCKLING LOADS FOR PILES

While the containment vessel foundation mat is supported on piles on a bearing layer which, in WES' opinion, will not liquefy, these piles require lateral support above this layer to prevent buckling failure. If liquefaction occurs in some depth region along the pile, this support will be dimenished or absent. Further, as upward seepage from the liquefied zone develops, lateral support may be lost all the way from the zone to the base of the mat foundation. The Euler buckling load, P_{cr}, for a typical pile has been calculated as follows:

$$P_{cr} = \frac{2.05\pi^2 EI}{L^2}$$

where

E = Young's Modulus of the pile

I = Moment of inertia of the cross section about its neutral axis

L = Unsupported length

The following assumptions were made:

a. The pile was 9 in. in diameter. It actually had an 8 in. diameter at the tip and a 12 in. diameter at the butt.

b. The pile was made of a linear elastic material with a Young's Modulus of 3,000,000 psi. It actually was made of 3500 psi, 28-day strength, cast in-place concrete inside a thin steel shell.

c. The pile was fixed at the base of the mat foundation.

d. The pile was pinned at a depth, L , below the base of the mat.

For these assumptions, the relation of P_{cr} to L is shown on Figure A1.

These piles have been rated in Reference 10 to have a 50-ton static load capacity. Presumably, the piles have vertical loads considerably less than this value. At the rated load, the analysis indicates that the unsupported length at which buckling would take place is approximately 40 ft. On Figure 14 of the main text, the vertical distance from the mat to the bottom of the shaded zone is 24 ft or less. The piles appear capable of supporting their vertical working loads even if lateral support is lost in this region. However, there are also horizontal dynamic loads that act on the pile butts as a result of earthquake excitation which tend to bend the piles in themselves and make the vertical loads eccentric which would in turn cause further bending. Some rough calculations suggest that the bending capacity of the piles is low with respect to the moments which might occur. A more thorough investigation of the dynamic bending problem is a complex but tractable structural dynamics problem beyond the scope of this study.

For the 0.2 g loading there is no point in performing such an analysis as Figure 15 of the main text indicates a possible unsupported length of over 80 ft. If loss of lateral support should occur over this length, as shown on Figure A1, the pile would buckle under its static load alone.

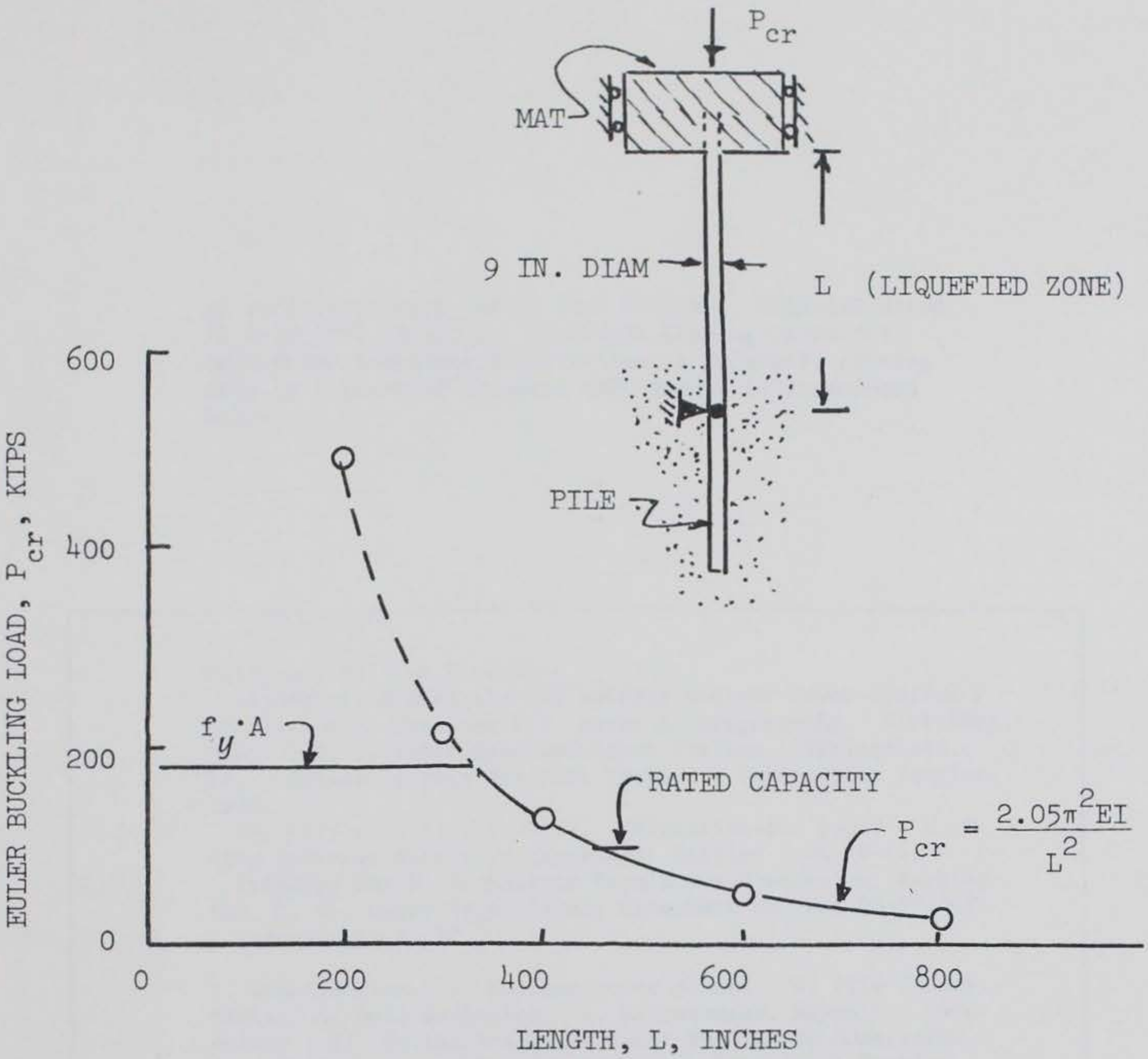

Figure A1. Buckling Resistance Versus Length of Unsupported Zone